Published by Institute of Physics Publishing for SISSA/ISAS
Received: *August 02, 2002*
Accepted: *August 05, 2002*

Measuring R-parity-violating couplings in dilepton production at the LHC

Debajyoti Choudhury
HarishChandra Research Institute
Chhatnag Road, Jhusi, Allahabad 211 019, India
E-mail: debchou@mri.ernet.in

Rohini M. Godbole*
Theory Division, CERN, Geneva 23, Switzerland
E-mail: Rohini.Godbole@cern.ch, rohini@cts.iisc.ernet.in

Giacomo Polesello
INFN, Sezione di Pavia
Via Bassi 6, Pavia 27100, Italy
E-mail: Giacomo.Polesello@cern.ch

Abstract: We revisit the issue of probing R-violating couplings of supersymmetric theories at hadronic colliders, particularly at the LHC. Concentrating on dimuon production, an evaluation of the optimal sensitivity to the R-violating coupling is performed through a maximum likelihood analysis. The measurement uncertainties are evaluated through a study of fully generated events processed through a fast simulation of the ATLAS detector. It is found that a host of R-violating couplings can be measured to a statistical accuracy of better than 10%, over a significant part of the $m_{\tilde{f}} - \lambda$ parameter space still allowed by low energy measurements. Since the bounds thus obtained do not simply scale as the squark mass, one can do significantly better at the LHC than at the Tevatron. The same analysis can also be extended to assess the reach of the LHC to effects due to any non-SM structure of the four-fermion amplitude, caused by exchanges of new particles with different spins such as leptoquarks and gravitons that are suggested by various theoretical ideas.

Keywords: Supersymmetry Phenomenology, Hadronic Colliders.

*Centre for Theoretical Studies, Indian Institute of Science, Bangalore 560 012, India

JHEP08(2002)004

Contents

1. Introduction

Within the Standard Model (SM), electroweak gauge invariance ensures the conservation of both lepton number and baryon number, at least in the perturbative context. However, this is not so within the Minimal Supersymmetric Standard Model (MSSM). The most general superpotential respecting the gauge symmetries of the SM contains bilinear and trilinear terms which do not conserve either the baryon number (B) or the lepton number (L). Clearly, the simultaneous presence of both lepton- and baryon-number-violating operators could lead to very rapid proton decay, especially for TeV scale sparticle masses. The existence of all such terms can be forbidden by postulating a discrete symmetry [1, 2], called R-parity, which implies a conserved quantum number $R_p \equiv (-1)^{3B+L+S}$, where S stands for the spin of the particle. The very definition implies that all the SM particles have $R_p = +1$, while all the superpartners are odd under this symmetry. Thus, apart from suppressing proton decay, it also guarantees the stability of the lightest supersymmetric particle (LSP), thereby offering a ready-made candidate for cold dark matter.

However, while a conserved R-parity seems desirable, it is perhaps too strong a requirement to be imposed. For one, the measure is an *ad hoc* one and there does not exist an overriding theoretical motivation for imposing this symmetry, especially since a suppression of the proton decay rate could as well be achieved by ensuring that one of B and

JHEP08(2002)004

L is conserved. Indeed, it has been argued [3] that this goal is better served by imposing a generalized baryon parity instead. Unlike R-parity, this latter (Z_3) symmetry also serves to eliminate dimension-5 operators that could potentially have led to proton decay. Furthermore, non-zero $\not{R}_p$ couplings provide a means of generating the small neutrino masses that the neutrino oscillation experiments seem to call for. Similarly, a significant value for such couplings has been shown to provide respite from the tachyonic nature of sleptons in models with anomaly-mediated supersymmetry breaking [4]. It is thus of both theoretical and phenomenological interest to consider violations of R-parity.

Limiting ourselves to a renormalizable superpotential, the possible R_p-violating terms can be parametrized as

$$W \supset \sum_i \kappa_i L_i H_2 + \sum_{i,j,k} \left(\lambda_{ijk} L_i L_j E^c_k + \lambda'_{ijk} L_i Q_j D^c_k + \lambda''_{ijk} U^c_i D^c_j D^c_k, \right) , \tag{1.1}$$

where i, j, k are generation indices, L (Q) denote the left-handed lepton (quark) superfields, and E^c, D^c and U^c are the right-handed superfields for charged leptons, down and up-type quarks, respectively. The couplings λ_{ijk} and λ''_{ijk} are antisymmetric in the first and the last two indices, respectively. A conserved baryon number requires that all the λ''_{ijk} vanish identically, thereby avoiding rapid proton decay.

As with their R_p-conserving cousins, namely the usual Yukawa couplings, these couplings are entirely arbitrary. Some phenomenological constraints exist, though. For example, the preservation of a GUT-generated $B - L$ asymmetry necessitates the preservation of at least one of the individual lepton numbers over cosmological time scales [5]. At a more prosaic level, the failure of various collider experiments [6] to find any evidence of supersymmetry[1] has implied constraints in the parameter space. Even for superpartners too heavy to be produced directly, strong bounds on these couplings can be inferred from the remarkable agreement between low energy observables and the SM predictions. These include, for example, meson decay widths [9, 10], neutrino masses [10, 11], rates for neutrinoless double beta decay [12], etc. The bounds generally scale with the sfermion mass and, for $m_{\tilde{f}} = 100\,\mathrm{GeV}$, they range from ~ 0.02 to 0.8 [13].

In general, therefore, when one studies the collider signals for R_p-violating supersymmetry, it is usual to consider the so-called "weak" R_p-violation scenario where the production of the superparticles goes through gauge couplings and the only role of R_p-violation is in the decay of the lightest supersymmetric particle [14]. Such studies are clearly insensitive to the exact size of the R_p-violating coupling as long as it is large enough to make the decay length of the LSP undetectable.[2] The processes that are directly sensitive to the size of this R_p-violating coupling are the production of sparticles through them [7, 16], the decays of sparticles through them [17, 18] or through indirect effects of the virtual sparticle exchange by interference of the R_p-violating amplitude with the SM one [17] and [19]–[22].

[1]Although R-parity violation has been touted as an explanation [7] for the reported excess of high-Q^2 events at HERA [8], it is no longer clear that this anomaly persists.

[2]If any of the R_p-violating couplings is $> 10^{-6}$ or so, then the LSP will decay within the detector [15].

An inspection of the aforementioned low-energy constraints shows that they are strongest when the term involves only the first two generations, and are often rather weak when one or more of the superfields belong to the third generation. In the context of collider experiments, a measurement of such couplings could, in principle, be done in more than one way, e.g. direct production, the decays of particles such as the top quark or sparticles other than the LSP through $\not{R}_p$ coupling, as well as through virtual exchanges. For example, in the event of a large coupling, one could study the rate for the production of a single superparticle. However, such measurements are subject to uncertainties from the luminosity measurement in some cases and also from the knowledge of branching ratios. We therefore revisit the issue of the indirect determination of some of the λ'_{ijk} couplings at the LHC, using their contribution to the production of lepton pairs.

Clearly, for such contributions to be significant, the initial state must involve quarks of the first generation or, in other words, at least one of j and k must be 1. Restricting ourselves, for the sake of definiteness, to muons in the final state, one sees that the least constrained among the relevant couplings [13] are λ'_{231} and λ'_{211}. We look at the reach of the LHC in the two-dimensional $\lambda' - m_{\tilde{q}}$ plane. The current study goes much beyond the earlier analyses of this process [19, 21] at the Tevatron in that we exploit the differences in the angular distribution of the leptons as well as the invariant mass distribution of the lepton pair. The use of this additional information increases the sensitivity to the R_p-violating couplings. Through a detailed experimental analysis, we show that it should be possible to keep the systematic uncertainties at the level of a few per cent. We further find that this analysis would serve a role complementary to that played by looking for $\not{R}_p$-violating decays of the squarks.

The rest of the article is planned as follows. In the next section, we first outline the details of the production of $\mu^+\mu^-$ pairs at the LHC along with the discriminatory features of the various distributions we use. We present the result of a parton-level calculation in this discussion. Following it up are the details of the maximum likelihood analysis technique used by us, and we present the results of the same at the parton level as well as at the level of fully generated events. We then give a discussion of the various systematic uncertainties in the analysis. After this, we briefly discuss the R_p-violating branching ratios of the third-generation squark. We show that for the squark mass range considered in this paper, there exists a region in parameter space in which the λ'_{231} coupling could in principle be measured at the 5% level at LHC at full luminosity. This demonstrates the above mentioned complementarity very nicely.

2. Drell-Yan in the presence of R_p violation

The Drell-Yan process at a hadronic collider has, over the years, been studied in great detail. Its analysis has served as an excellent theoretical laboratory, first for the quark parton model and later for perturbative QCD. In fact, not only the NLO, but even the NNLO corrections have been computed [23]. In the context of the present analysis, though, we shall limit ourselves to leading-order calculations. The reasons are manifold. For one, the NNLO calculations, within the SM, have demonstrated that a constant K-factor gives a very good description of the corrections over a very wide range of kinematic variables. Secondly, the radiative corrections in the presence of non-SM physics, such as the case under study, have not yet been calculated. It might be argued, though, that since we are interested in probing typically small $R\!\!\!/_p$ couplings, a very precise calculation of the strong corrections to these additional contributions is not crucial. Instead, we might assume that the K-factor is essentially the same as in the SM. Clearly, this estimate is quite a reasonable one; it is supported by the recent calculations [24] of K-factors for chargino or neutralino pair-production, each of which receives t-channel contributions as in the present case. This assumption simplifies the analysis, as the Born term is extremely simple to analyse.

A look at the superpotential given by eq. (1.1) tells us that it is only the λ'_{ijk} couplings that can affect Drell-Yan production of a dilepton pair. Expressed in terms of the component fields, the relevant part of the lagrangian reads

$$\begin{aligned}\mathcal{L}_{\lambda'} = \lambda'_{ijk}\Big[&\tilde{\nu}^i_L \bar{d}^k_R d^j_L + \tilde{d}^j_L \bar{d}^k_R \nu^i_L + (\tilde{d}^k_R)^* (\bar{\nu}^i_L)^c d^j_L - \\ &- \tilde{e}^i_L \bar{d}^k_R u^j_L - \tilde{u}^j_L \bar{d}^k_R e^i_L - (\tilde{d}^k_R)^* (\bar{e}^i_L)^c u^j_L\Big] + \text{h.c.}\end{aligned} \tag{2.1}$$

A non-zero λ'_{2jk} would then lead to an additional u-channel ($\tilde{d}^k_R$ exchange) diagram for the process $\bar{u}_j u_j \to \mu^- \mu^+$ and a t-channel ($\tilde{u}^j_L$ exchange) diagram for $\bar{d}_k d_k \to \mu^- \mu^+$. Note that neither resonance production processes leading to the dimuon final state nor processes such as $q_i \bar{q}_j \to e^- \mu^+$ can occur when only a single $R\!\!\!/_p$ coupling is non-zero, an assumption [25] that we shall work with.

The differential cross section is modified in a straightforward way and reads, in the centre of mass of the $\mu^+\mu^-$ system, as

$$\begin{aligned}\frac{\mathrm{d}\hat{\sigma}}{\mathrm{d}\cos\theta}[q\bar{q} \to \mu^-\mu^+] = \frac{\pi\alpha^2 \hat{s}}{24}\Big\{&(1+\cos\theta)^2 \left[|f^s_{LR}|^2 + |f^s_{RL}|^2\right] + \\ &+ (1-\cos\theta)^2 \left[|f^s_{LL}|^2 + |f^s_{RR}|^2\right]\Big\},\end{aligned} \tag{2.2}$$

$$f^s_{LR} = -\frac{Q^q}{\hat{s}} + \frac{g^q_L g^e_L}{\hat{s} - m_Z^2 + i\Gamma_Z m_Z}, \tag{2.3}$$

$$f^s_{RL} = -\frac{Q^q}{\hat{s}} + \frac{g^q_R g^e_R}{\hat{s} - m_Z^2 + i\Gamma_Z m_Z}, \tag{2.4}$$

$$f^s_{LL} = -\frac{Q^q}{\hat{s}} + \frac{g^q_L g^e_R}{\hat{s} - m_Z^2 + i\Gamma_Z m_Z} - \frac{1}{2}\frac{(\lambda'_{2jk}/e)^2}{\hat{u} - m^2_{\tilde{d}_{kR}}}\delta_{qu_j}, \tag{2.5}$$

$$f^s_{RR} = -\frac{Q^q}{\hat{s}} + \frac{g^q_R g^e_L}{\hat{s} - m_Z^2 + i\Gamma_Z m_Z} + \frac{1}{2}\frac{(\lambda'_{2jk}/e)^2}{\hat{t} - m^2_{\tilde{u}_{jL}}}\delta_{qd_k}, \tag{2.6}$$

where Q^f represents the charge of the fermion f and $g^f_{L,R}$ its couplings to the Z. Clearly, the new contribution is relevant only if $q = u, d$ or, in other words, only if at least one of j and k refers to the first generation. Of the nine $R\!\!\!/_p$ couplings that could, in principle, contribute to dimuon production, we thus need to concern ourselves with only five.

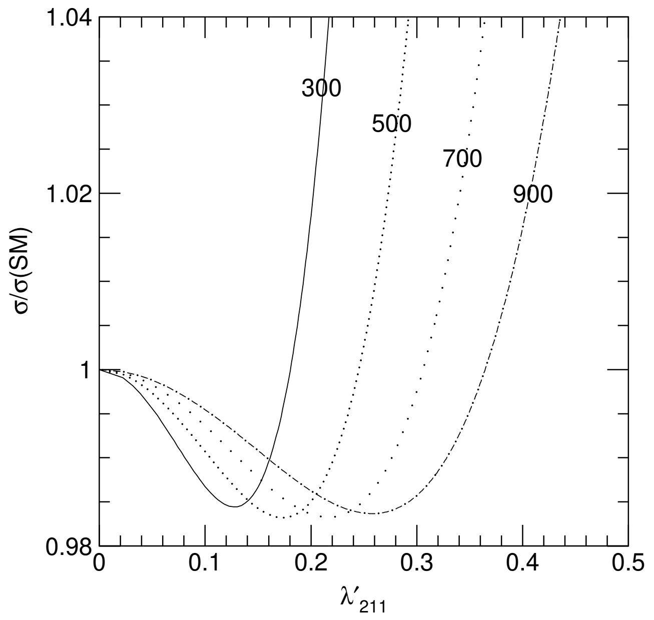

Figure 1: Relative change of the dimuon cross section at the LHC as function of the coupling λ'_{211}. The assumed lower limit on the dilepton invariant mass is 500 GeV. The curves correspond to four different squark masses: 300, 500, 700 and 900 GeV, respectively.

For a given strength of the coupling, the change wrought in the total cross section would depend on the mass of the squark(s) involved as well as on the particular subprocess that is being affected.

In figure 1, we present the relative deviation of the total cross section for a particular coupling, i.e. λ'_{211}, and different values of the squark masses (for convenience, we assume that $\tilde{u}_L$ and $\tilde{d}_R$ are degenerate). The lower cut on the dilepton invariant mass assumed for the calculation is 500 GeV. As far as the total cross section is concerned, the difference is only at the level of a few per cent, even for moderately large values of the coupling. However, this is somewhat misleading, since the deviation from the Standard Model increases with the dilepton mass, and therefore the observed integrated effect strongly depends on the lower limit on the dilepton mass taken for the calculation. The extra contributions manifest themselves more markedly in the kinematic distributions, modifying them from those expected within the SM in three essential ways: (1) enhanced cross section for high $\ell^+\ell^-$ invariant mass, (2) different lepton angular distribution in the $\ell^+\ell^-$ rest frame and (3) different boost distribution of the $\ell^+\ell^-$ system.

For a given point in the supersymmetric parameter space, these differences are demonstrated in figure 2. The figure shows distributions in the invariant mass M of the dimuon pair, the difference in the rapidities of the two leptons $\Delta\eta$ and the rapidity of the pair itself $\eta_{\rm pair}$. Clearly, the use of the differential distributions would result in an enhanced sensitivity with respect to just the event rate comparison of figure 1. Note the substantial broadening of the distribution in M. In fact, rather than limiting ourselves to a study of a distribution in one of the three independent variables listed above, it is conceivable that the use of the full kinematic information, taking into account the correlation of the kinematic

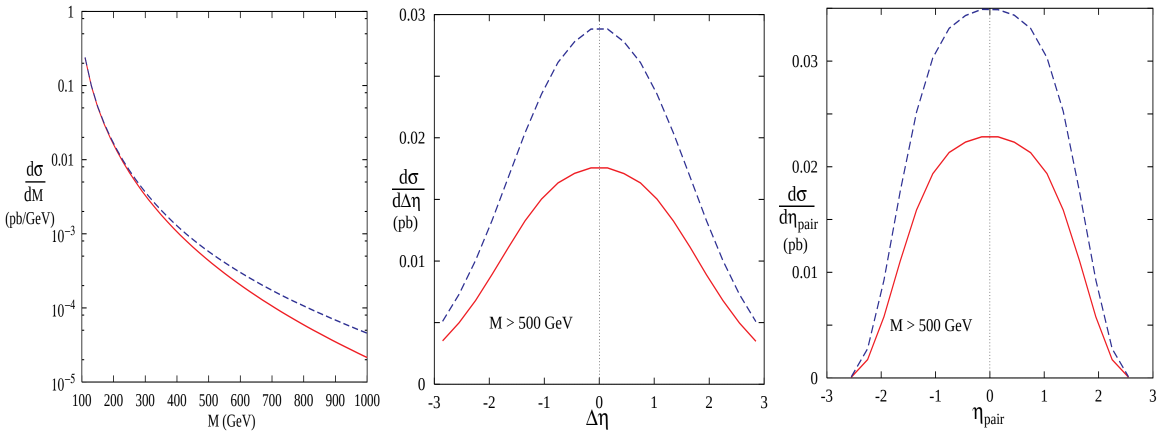

Figure 2: The phase-space distributions for the Drell-Yan process at the LHC. We have demanded that the $\mu^{\pm}$ have a minimum transverse momentum of 50 GeV each and be within the pseudorapidity range $-3 < \eta < 3$. For the rapidity distributions, an additional cut ($M > 500\,\mathrm{GeV}$) has been imposed. In each case, the lower curve corresponds to the SM and the upper curve to $\lambda'_{211} = 0.5$, $m_{\tilde{q}} = 800\,\mathrm{GeV}$.

variables, would be even more powerful. In the next two sections we discuss how exactly we propose to do this, albeit with a choice of independent variables slightly different from that mentioned above.

3. Maximum likelihood method

Our goal, then, is to exploit to the full the differences in the kinematic distribution of the $\mu^+\mu^-$ pair caused by the presence of the $\not{R}_p$ interactions. Such a study is expected to yield a measurement (or at least constraints) in the two-dimensional supersymmetric parameter space, namely the mass-coupling plane. The problem of simultaneous determination of these two, viz. λ' and $m_{\tilde{q}}$, is the classical problem of parameter estimation. In view of the systematic uncertainties (experimental due to the luminosity and theoretical due to parton distributions, K-factors, etc.) in the normalisation of the signal, it is best to use the maximum likelihood method, which does not require a precise knowledge of the absolute size of the signal, but only that of its shape.

As figure 2 shows, the fall-off in the invariant mass distribution is indeed substantially slower for the R_p-violating (RPV) contribution. For the other distributions too, the difference is quite discernible. However, instead of using the variables of figure 2, we choose to work with an equivalent (independent) set, namely the momentum fractions x_1 and x_2 of the initial-state partons and the cosine of the scattering angle, $\cos\theta$. Neglecting the transverse momentum of the $\mu^+\mu^-$ system, the event kinematics for a given event i is completely specified by these three variables. The log likelihood function is defined as:

$$\ln \mathcal{L} = \sum_{i=1}^{N_{\rm ev}} \ln F\left(\lambda', m_{\tilde{q}}, x_1^i, x_2^i, \cos\theta^i\right), \tag{3.1}$$

with F given by:

$$F = \frac{1}{\sigma(\lambda', m_{\tilde{q}})} \frac{d\sigma}{dx_1 dx_2 d\cos\theta} \left(\lambda', m_{\tilde{q}}, x_1^i, x_2^i, \cos\theta^i\right) . \qquad (3.2)$$

The cross section $\sigma(\lambda', m_{\tilde{q}})$ in the denominator is the one obtained *after* imposing all the analysis cuts. The latter, of course, are chosen so as to maximize the RPV contribution in the signal. The best estimate of the true values of the two parameters is then given by the particular pair $(\lambda', m_{\tilde{q}})$ that maximizes $\log \mathcal{L}$ for a given data sample. In addition to the advantage that comes from using only the shape of distributions as mentioned above, this method also has the good features of not requiring any binning, as well as exploiting the correlations among the different variables optimally. We note here that the objective of avoiding the systematic (both theoretical and experimental) errors due to the imprecision in the knowledge of the absolute size of the signal, could, in principle, also be achieved by comparing the size of the dimuon signal with the dielectron one. However, the latter method presupposes that no unknown physics effects exist in the dielectron mass spectrum and hence it is not completely model-independent. Furthermore, the comparison of two different spectra involves the compounding of errors, thereby affecting the accuracy adversely.

4. Data analysis

For our analysis of the simulated data, we first generate events corresponding to an integrated luminosity of $100\,\mathrm{fb}^{-1}$, which corresponds to a year of LHC operation in its high luminosity mode. The evaluation of the achievable sensitivity in the λ' measurement requires the generation of many times the statistics expected for a single experiment, for a fine grid on λ' for a few values of $m_{\tilde{q}}$. The parton-level generation of unit weight events without initial-state QCD showering is about ten times faster than the generation of full PYTHIA [26] events followed by the fast detector simulation for the ATLAS detector [27]. We will therefore first evaluate the statistical sensitivity of the experiment at the parton level. The results thus obtained will then be compared with the same procedure applied to fully generated events for a few selected points in parameter space, in order to evaluate the effect on the experimental sensitivity of the experimental smearing and of the introduction of initial-state QCD radiation.

We select events with two isolated opposite-sign muons, satisfying the following two requirements: 1) $P_T^\mu > 10\,\mathrm{GeV}$, $|\eta_\mu| < 2.5$ and 2) $m_{\mu^+\mu^-} > 500\,\mathrm{GeV}$. The first criterion essentially ensures that the muons are visible in the detector. The invariant-mass cut, on the other hand, is motivated by the observation that the relative deviation of the cross section starts to become significant only at $m_{\mu^+\mu^-} \sim m_{\tilde{q}}$ [19]. The optimal choice of the cut is determined not only by the squark mass under consideration, but also by the total number of events (in other words, the luminosity). However, rather than working with a squark mass-dependent cut, we choose to adopt the simpler strategy of a fixed choice for the invariant-mass cut. Approximately 7500 events survive these cuts for our choice of the luminosity.

As is clear from the definition of the likelihood function, a complete knowledge of the kinematics of the event is necessary for its calculation. However, it must be borne in mind

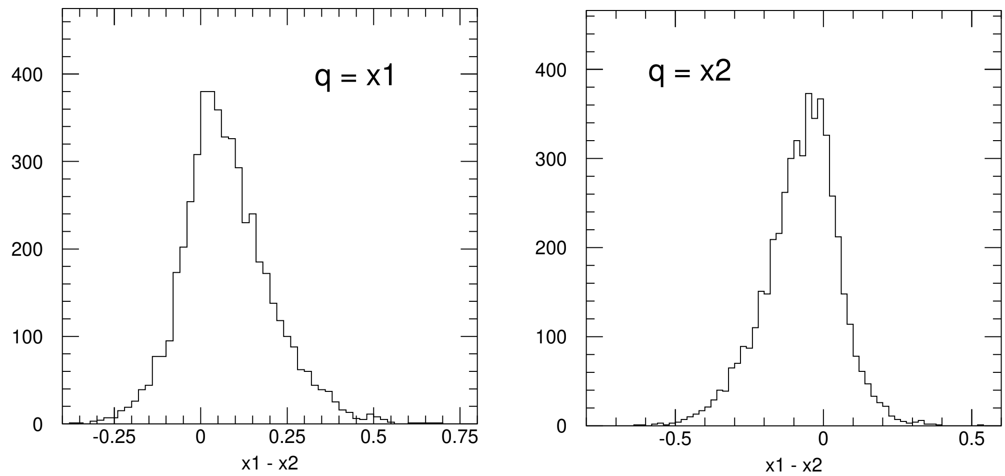

Figure 3: Difference $x_1 - x_2$ when the quark is picked up from the proton labelled "1" (left plot) and "2" (right plot).

that, at a pp collider such as the LHC, it is not possible to know for certain the initial direction of the quark (in the $\bar{q}q$ hard scattering subprocess). Hence, only the absolute value of $\cos\theta$ is measurable, not the sign. Part of this information can, however, be recovered, by using the knowledge of x_1 and x_2 and the fact that, in the proton, the x distribution for valence quarks is harder than for antiquarks. Arbitrarily labelling the proton beams "1" and "2", the difference $x_1 - x_2$ can be inferred from the longitudinal momentum of the dimuon pair.

In figure 3 we show the distribution of $x_1 - x_2$, when the quark is picked up from the proton labelled "1" (left plot) and "2" (right plot). It can be clearly seen that in most cases the quark is taken from the side with higher x. To make use of this information, the likelihood is built by summing the functions F calculated for both signs of $\cos\theta$, weighted by the probability, for the given (x_1, x_2) combination that the quark is in proton "1" or "2".

4.1 Parton level analysis

For the sensitivity study, we generated a grid of points with different values of λ' (with a spacing of 0.025) for four different equispaced values of the squark mass ranging from 300 to 900 GeV. For each point, 5×10^5 events with unit weight were generated. The likelihood was calculated in steps of λ'^2 for $-0.05 \leq \lambda'^2 \leq 0.2$. The inclusion of the unphysical range is necessary for the evaluation of the confidence interval. If the likelihood function has a local maximum for a positive (physical) λ'^2, we take this value as *a measurement*. Otherwise, we take the absolute maximum, even though it may be in the unphysical (negative) region. The cross section being a quadratic function of λ'^2, a secondary maximum may appear, and often does for negative λ'^2. In fact, even for λ'^2 values large enough for the experiment to be sensitive to squark exchange, a small fraction of the Monte Carlo experiments can show the unphysical maximum to be higher than the physical one. This feature is illustrated in figure 4, where we display the likelihood as a function of λ'^2_{211} for four experiments, assuming

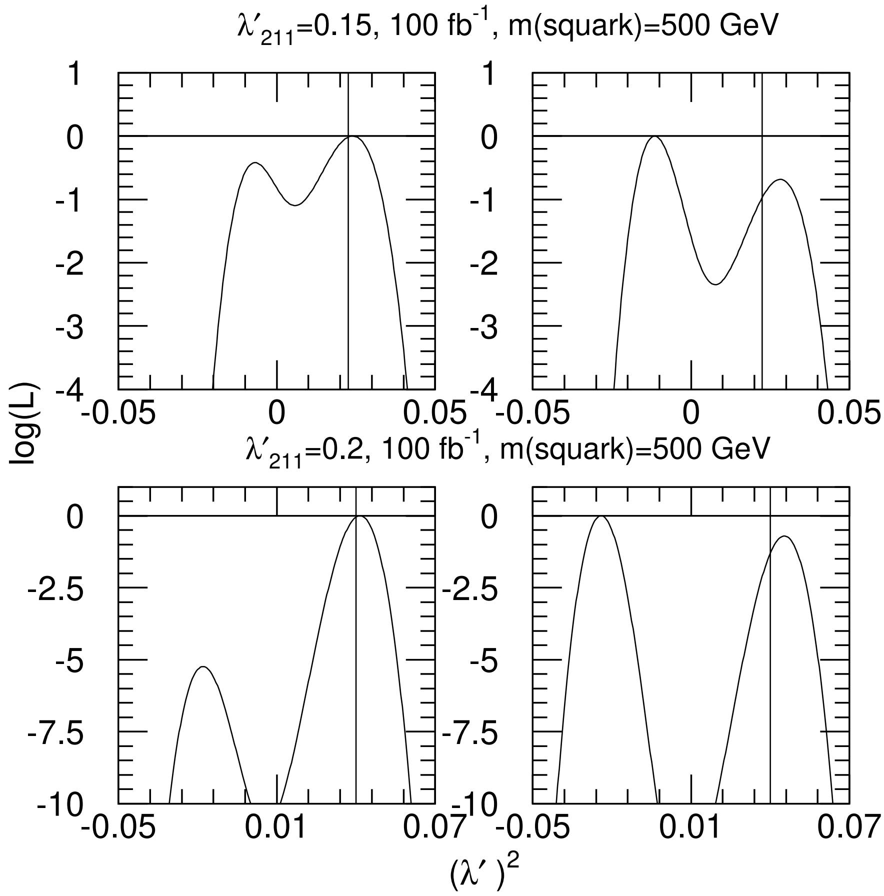

Figure 4: Shape of the log likelihood function as a function of λ'^2_{211} for four different Monte Carlo experiments. The value of λ'_{211} used in the generation of events, shown as a vertical line, is 0.15 for the upper plots, and 0.2 for the lower plots. The assumed squark mass is $m_{\tilde{q}} = 500\,\text{GeV}$. The integrated luminosity is $100\,\text{fb}^{-1}$.

$m_{\tilde{q}} = 500\,\text{GeV}$. The upper plots are for $\lambda'_{211} = 0.15$, which is below the experimental sensitivity for this particular squark mass. In this case, even when the physical maximum is found, the dip between the two maxima is shallow ($1\sigma \sim \Delta \ln \mathcal{L} = 0.5$), and very often the absolute maximum occurs at a negative λ'^2. The lower plots are for $\lambda'_{211} = 0.2$. The two maxima here are always well separated; the rare cases when the absolute maximum is in the unphysical region correspond to experiments for which the positive maximum is somewhat displaced from the nominal value.

In order to evaluate the uncertainty on the λ' measurement, we generated $\sim$ 1500 Monte Carlo experiments for an integrated luminosity of $100\,\text{fb}^{-1}$; for each of them we calculated the maximum of the likelihood function according to the above prescription. Since the generated statistics is only $\sim$ 70 times the statistics for a single experiment, each of the Monte Carlo experiments was produced by randomly picking, inside the available statistics, the $\sim$ 7500 events corresponding to one year of running. With this procedure each event is used for $\sim$ 25 Monte Carlo experiments.

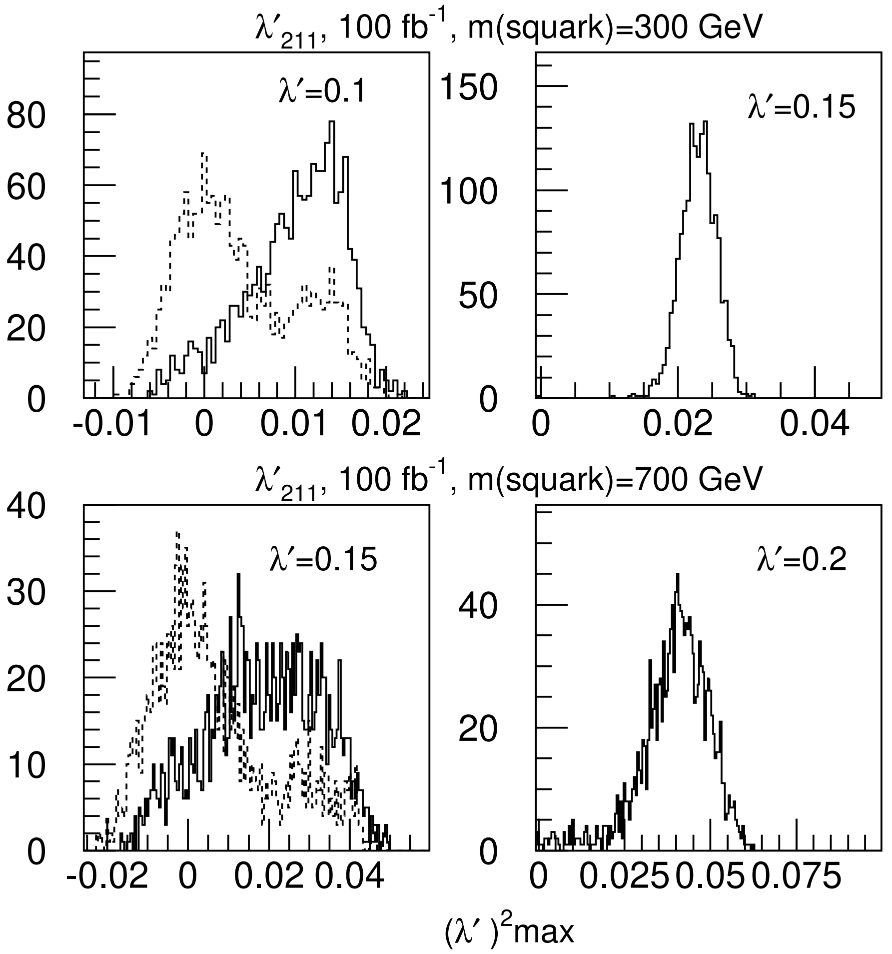

Figure 5: Distribution of the λ'^2_{211} value estimated through the maximization of the likelihood function for a set of $\sim$ 1500 Monte Carlo experiments. The upper (lower) set corresponds to a squark mass of 300 (700) GeV. For each case, we show the distributions for three values of λ' used in the generation of events: 0 (dashed line), a value below the experimental sensitivity for the assumed squark mass and integrated luminosity (left plot, full line), and a value for which a good λ measurement is achievable (right plot). The integrated luminosity is $100\,\mathrm{fb}^{-1}$.

A common behaviour is observed for all four squark masses considered. For values of λ'^2 approximately up to the minimum in the cross section shown in figure 1, the distribution of the estimated values of λ'^2 is very broad, and extends up to a specific value of λ'^2, which depends on the mass, in such a way that the distribution of the measured λ'^2 becomes gaussian only for λ'^2 values above this. This means that the experiments start being sensitive to the effect somewhere in this transition region. Figure 5 shows the results for $m_{\tilde{q}} = 300$ and 700 GeV.

4.2 Evaluation of experimental sensitivity

We follow here the frequentist approach of [28], where the sensitivity of an experiment is defined as: "the average upper limit that would be obtained by an ensemble of experi-

JHEP08(2002)004

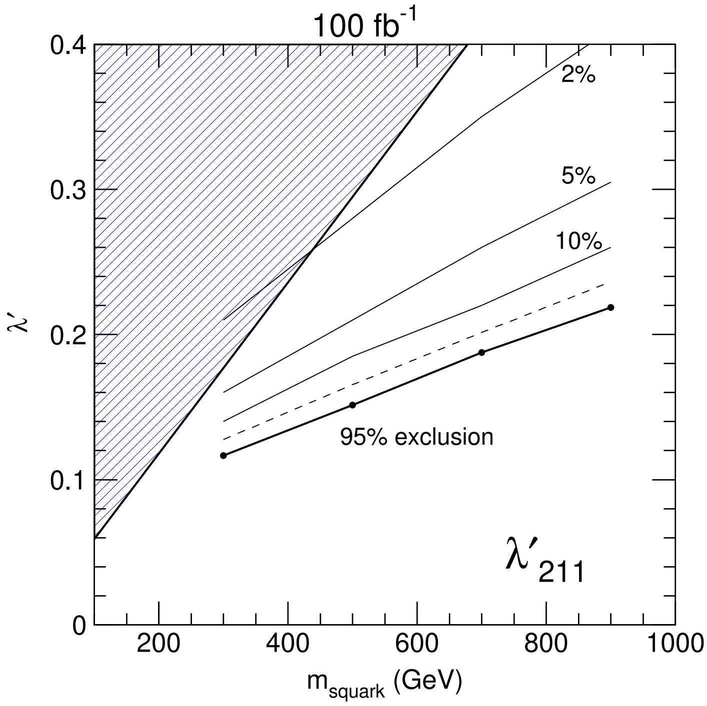

Figure 6: 95% sensitivity region in the $m_{\tilde{q}} - \lambda'$ plane for an integrated luminosity of $100\,\mathrm{pb}^{-1}$. The dashed line corresponds to the choice of the central interval in the Neyman construction. The analysis is performed at the parton level. The contours corresponding to an uncertainty on λ' of 2, 5 and 10% (under the assumption of perfectly known squark mass) are also shown. The shaded region on the left is excluded by low energy measurements.

ments with the expected background and no true signal". For each considered value of the squark mass, we build, therefore, confidence belt according to the Neyman construction. We adopt as the auxiliary choice for the definition of the belt the one leading to "upper confidence intervals", defined by [28, eq. (2.5)]. For an ensemble of experiments with $\lambda = 0$, we then calculate the respective upper limits using the confidence belt thus built, and then take the average. The results are shown on the $(m_{\tilde{q}} - \lambda')$ plane in figure 6, together with the region corresponding to the bounds on λ'_{211} from low-energy processes. If no signal is present in the data, the result of the experiment will be the exclusion of the region in the $(m_{\tilde{q}} - \lambda')$ plane above the curve labelled "95% exclusion". If a signal is present, the experiments will be able to extract a measurement of the λ' couplings. The assessment of the precision of this measurement depends on the available information on $m_{\tilde{q}}$, and on the dependence of the measured value of λ' on the assumed squark mass. As a first, unrealistic, approximation we show in figure 6 the curves in the $(m_{\tilde{q}} - \lambda')$ plane corresponding to a statistical uncertainty on λ' of 2, 5 and 10%, respectively, if no error is assumed on the squark mass.

It is interesting to consider the dependence of the error estimate on the available prior information on the squark mass. Consider the pair-production of the said squark at the LHC. For the range of values of the λ' couplings addressed in this paper, every

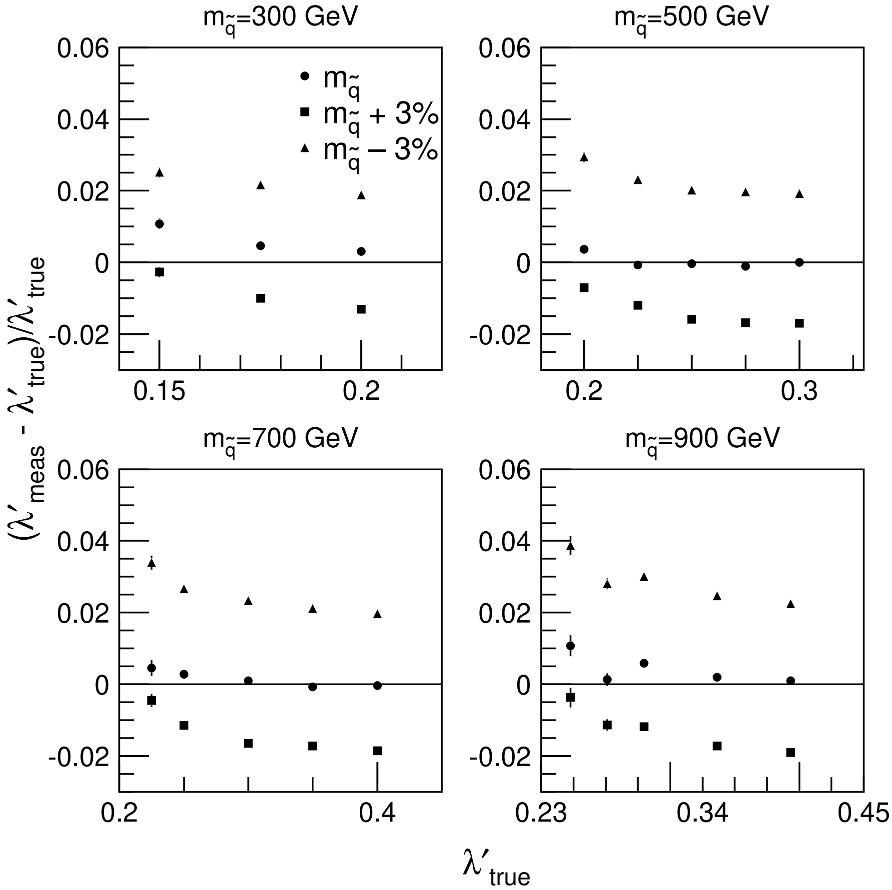

Figure 7: Fractional deviation of the measured λ' value from the true one as a function of λ' for three values of the squark mass used in the likelihood calculation: the nominal one (dots), reduced by 3% (squares), augmented by 3% (triangles). The four plots are respectively, for the four squark masses considered in the analysis, $m_{\tilde{q}} = 300, 500, 700$ and $900\,\mathrm{GeV}$.

supersymmetric event will contain two $\tilde{\chi}_1^0$ decaying into two jets and a muon or a muon neutrino. Detailed studies have shown that, in the ATLAS experiment, it will be possible to reconstruct the $\tilde{\chi}_1^0$ peak from its decay products, and, going up the decay chain, to reconstruct the squark masses [29]. The statistical precision of the mass measurement is essentially a function of the squark mass, and for squark masses below $\sim 1\,\mathrm{TeV}$, the error on the mass will be dominated by the systematic uncertainty on the reconstruction of the parton energy from the jet energy measurement. Such uncertainty is estimated to be approximately 3% in ATLAS [30]. Therefore, in the sensitivity region we have performed the λ' measurement for values of the squark mass displaced upwards and downwards by 3% with respect to the nominal mass. The results are shown in figure 7 for the four mass values considered in the analysis. The correlation between the λ' and $m_{\tilde{q}}$ measurement is positive, therefore a higher value of $m_{\tilde{q}}$ in input yields a higher λ' measurement. For the assumed value of the uncertainty on $m_{\tilde{q}}$, the additional uncertainty on λ' from this effect is of order 2–3% for all considered mass values. One can also observe from figure 7 that when the nominal mass value is used, the bias on λ' from the likelihood fit is less than 1%.

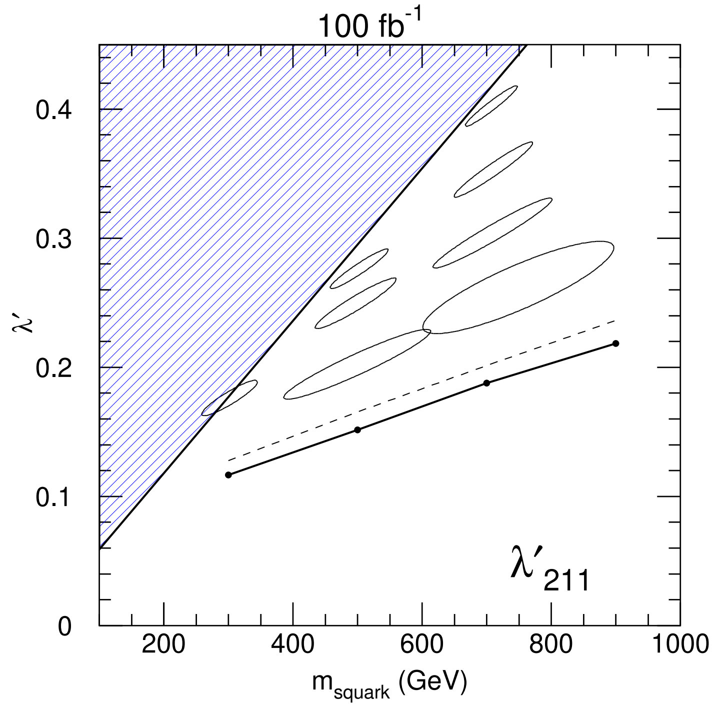

Figure 8: 1σ ellipses for the measurement of λ' and $m_{\tilde{q}}$ if no previous information on $m_{\tilde{q}}$ is assumed for different points in the $m_{\tilde{q}} - \lambda'$ plane and an integrated luminosity of $100\,\mathrm{pb}^{-1}$. The full and dashed lines correspond to the 95% exclusion region. The analysis is performed at the parton level. The shaded region on the left is excluded by low energy measurements.

Finally, we consider the combined precision, in the measurement of $m_{\tilde{q}}$ and λ', that may be achieved if a two-dimensional likelihood is used, and no prior information on the squark mass is assumed. We have performed this study for a few sample points, and the results are shown, in figure 8, as 1σ ellipses in the $(m_{\tilde{q}} - \lambda')$ plane, calculated on a sample of $\sim$ 500 Monte Carlo experiments. The resolution in mass is of the order of few tens of GeV, and quickly degrades when λ' approaches the edge of the sensitivity region. Given the correlation between the λ' and $m_{\tilde{q}}$ measurements, the λ' measurement is degraded accordingly. This statement is better quantified in table 1, where we give the parameters of the ellipses corresponding to $\log(\mathcal{L}_{\max}) - 1/2$ for the studied points, compared with the resolution on λ' if the squark mass is known. In particular, the parameter ρ, which measures the correlation of the two variables, is ~ 1, meaning that the variables are fully correlated. Thus, a combined measurement of squark mass and λ' is possible with this analysis for a significant fraction of the parameter space.

5. Analysis of fully generated events

The analysis in the previous section was performed assuming that the momentum of the $\mu^+\mu^-$ system has no component transverse to the beam axis, and that the muon momenta are perfectly measured in the detector.

$m_{\tilde{q}}$ (GeV)	λ'	$\sigma(\lambda')(1)$	$\sigma(\lambda')(2)$	$\sigma(m_{\tilde{q}})$ (GeV)	ρ
300	0.175	0.005	0.014	43	0.913
500	0.200	0.010	0.027	114	0.947
500	0.250	0.007	0.020	63	0.948
500	0.275	0.006	0.017	46	0.951
500	0.300	0.005	0.014	38	0.949
700	0.250	0.013	0.036	148	0.859
700	0.300	0.009	0.028	98	0.951
700	0.350	0.007	0.020	56	0.954
700	0.400	0.005	0.016	40	0.964

Table 1: Statistical errors on the λ' measurement for a few sample points. The value in the third column $[\sigma(\lambda')(1)]$ is the uncertainty assuming that the squark mass is known with zero error. The last three columns give the parameters of the 1σ ellipses for the two-dimensional likelihood on $(m_{\tilde{q}} - \lambda')$, where ρ is the correlation coefficient for $m_{\tilde{q}}$ and λ'.

In order to perform a more realistic evaluation of the precision of λ' measurement, achievable in a real experiment, the matrix elements for the squark exchange process have been inserted into the PYTHIA [26] event generator as an external process, and full events have been generated, including the full PYTHIA machinery for QCD showering from the initial-state quarks, and for the hadronization. The events thus generated have been passed through the fast simulation of the ATLAS detector [27], including, in particular, a very detailed parametrization of the resolution of the muon momentum measurement.

The values of x_1, x_2 have been inferred from the measured four-momenta of the detected muons, according to the formulae:

$$\frac{2\,P_L^{\mu^+\mu^-}}{\sqrt{s}} = x_1 - x_2\,, \qquad m^2_{\mu^+\mu^-} = x_1 x_2 s\,.$$

For the evaluation of $\cos\theta$ we use the Collins-Soper convention [31], which consists of an equal sharing of the $\mu^+\mu^-$ system transverse momentum between the two quarks. We show, in figure 9, the two-dimensional correlation between the generated and the reconstructed values for the variable x_1 as well as their ratio. Only events that pass the analysis criteria enter these plots. For x_1, the RMS deviation is $\sim 10\%$, and is completely determined by the muon momentum resolution. A comparable resolution is obtained for $|\cos\theta|$ (figure 10), but with significant tails due to the presence of a non-zero transverse momentum of the $\mu^+\mu^-$ system.

Samples of events were generated for four squark masses, 300, 500, 700 and 900 GeV, and for three values of λ' for each mass, chosen in each case in an interval of 0.1 in λ'^2, approximately covering the transition region where this analysis becomes sensitive to the RPV contribution for an integrated luminosity of $100\,\mathrm{fb}^{-1}$, as described in the previous section. We then applied to these samples the unbinned likelihood analysis, as for the parton-level events. The evolution of the likelihood distributions with λ' is nicely reproduced. In particular, the threshold behaviour of the sensitivity is still present. The

JHEP08(2002)004

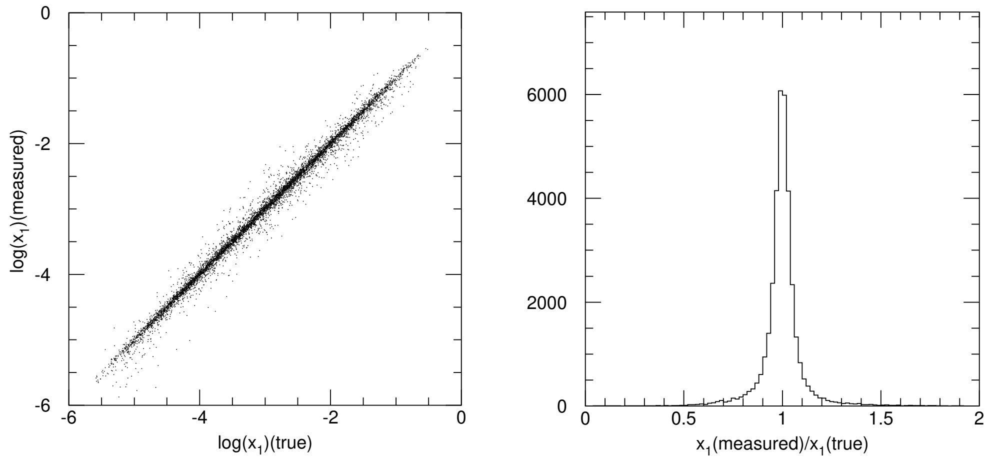

Figure 9: Left plot: correlation of the reconstructed value of $\log(x_1)$ with the generated value for a sample of events passing the analysis requirements. Right plot: distribution of the ratio of the reconstructed and generated value of x_1. The distributions are given for a sample of events passing the analysis cuts.

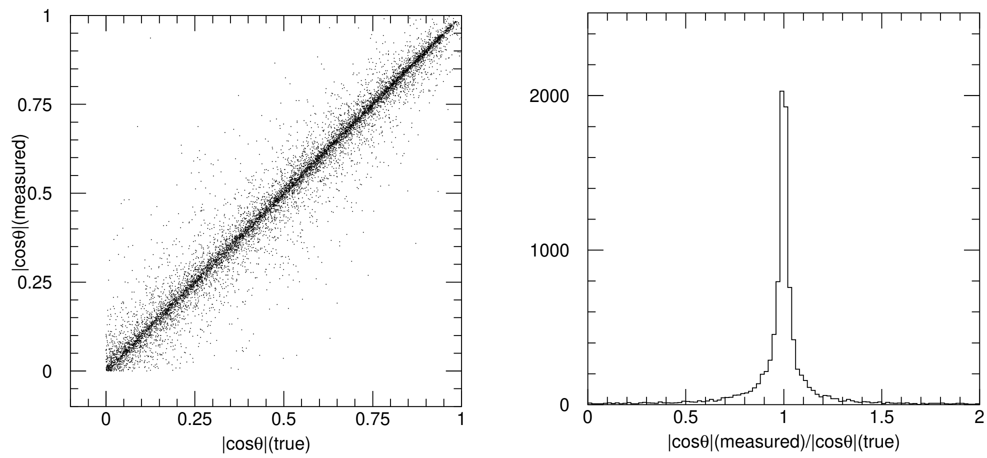

Figure 10: As in figure 9, but for $|\cos\theta|$.

distribution of the measured λ' is indeed dominated by the statistical performance of the maximum likelihood estimator, and not by the experimental resolution. The results of the analysis are shown in figure 11, for $m_{\tilde{q}} = 300\,\mathrm{GeV}$. Therefore, the sensitivity limit calculated at parton level, shown in figure 6, applies for the full event simulation as well. A difference is observed only for λ' values for which the distribution of the measured λ' for a set of Monte Carlo experiments is approximately gaussian. In this case, the presence of the experimental smearing induces a moderate increase in the λ' measurement resolution. Figure 12 shows a comparison of the achievable parton-level resolution with the corresponding experimental resolution. The four continuous lines give the estimated parton-level resolution for the four considered masses. Superimposed as data points are the resolutions obtained for the experimental simulation. A difference is observed mainly

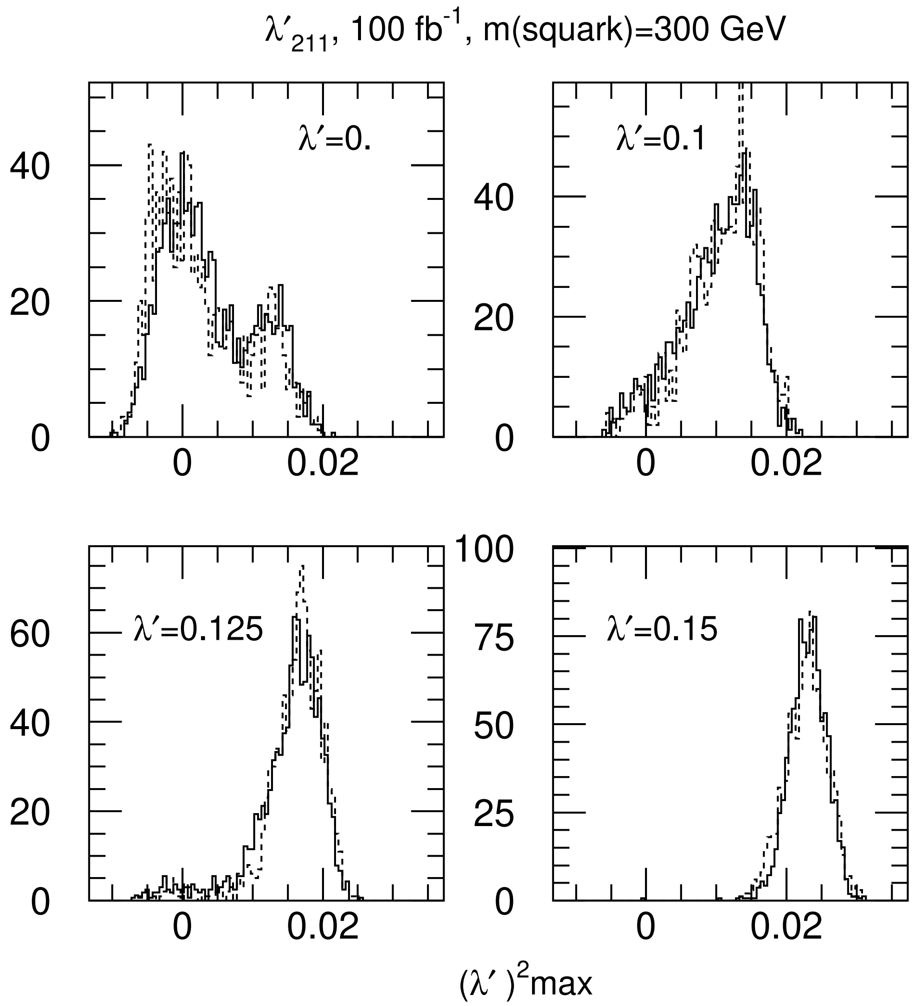

Figure 11: Distributions of measured λ'^2 for a set of Monte Carlo experiments for different values of λ' used for the generation of events. The full-line histograms are the parton-level distributions while the dashed histograms correspond to fully generated events.

for the lower λ' values, where the experimental simulation exhibits higher non-gaussian tails than the parton-level simulation, thus yielding a 10–20% higher RMS deviation. For higher λ' values, the resolutions are essentially identical. We can thus conclude that the curves shown in figure 6 are only marginally affected by the experimental uncertainties. This result is obtained under quite pessimistic assumptions. In fact, we use as a definition of F and its integral in eq. (3.2) the pure leading order formulas in eq. (2.6), without any attempt at parametrizing the $\mu^+\mu^-$ transverse momentum distribution.

In the analysis of real data, we also need to consider the backgrounds from non-Drell-Yan processes. The dominant background processes, for the invariant mass cut applied in this analysis, will be $\bar{b}b$, $\bar{t}t$, and WW production. For $\bar{b}b$ production the muons are not isolated, and we can apply lepton isolation, which consists of requiring an energy deposition of less than 10 GeV, not associated with the lepton in a pseudorapidity–azimuth $(\eta - \phi)$ cone of opening $\Delta R = 0.2$ around the lepton direction.

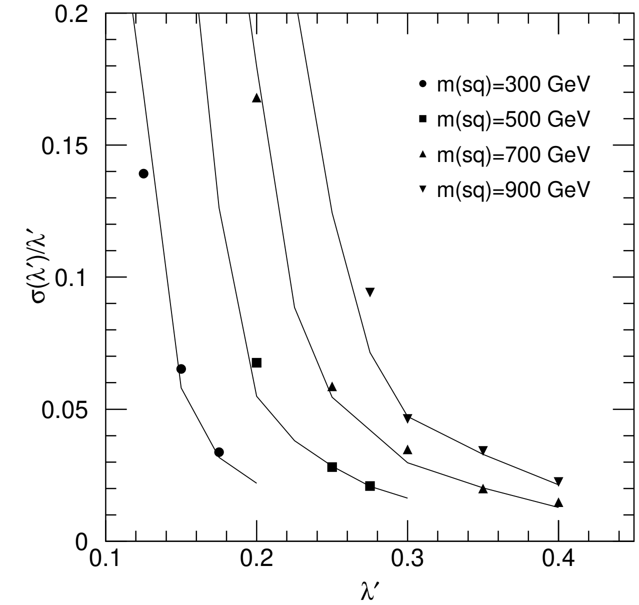

Figure 12: Curves of $\sigma(\lambda')/\lambda'$ as a function of λ' for an integrated luminosity of $100\,\text{fb}^{-1}$ and for four different squark masses. The full lines give the resolution obtained at parton level, and the points are the results of the full event simulation.

Without any additional cuts, for an integrated luminosity of $100\,\text{fb}^{-1}$, the backgrounds from $\bar{t}t$ and WW amount to ~ 1400 and ~ 500 events, respectively, for a signal of ~ 7400 events. The $\bar{t}t$ background can be strongly reduced by vetoing b-jets. We assume a tagging efficiency of 50% for a rejection factor of 100 (10) on light quark (charm) jets, respectively. This is appropriate for the high luminosity run. We also veto jets tagged as b-jets with $P_T > 30\,\text{GeV}$. The $\bar{t}t$ background is thus reduced to ~ 600 events, with negligible effect on the signal. Both for the $\bar{t}t$ and WW backgrounds, the events will have real E_T^{miss} from escaping neutrinos, and a further reduction can be achieved by vetoing on high E_T^{miss} events. This requirement, though, has a significant effect on the kinematics of signal events. In fact we are considering here high energy muons, for which the error in momentum measurement induces an instrumental imbalance in the vector sum of the lepton momenta, which grows with increasing momentum. Therefore the acceptance of any kinematic cut applied must be convoluted in the test function used for the likelihood in order to obtain the correct result. A complementary approach consists in accepting the relatively high level of background, and incorporating the background shape into the likelihood function. This should be possible with high precision, since the considered backgrounds yield twice as many $e\mu$ events as $\mu\mu$ events, allowing an estimate of the background level from the data themselves. The two approaches have different systematic uncertainties, and can be used in parallel, thus providing a double check on the result.

6. Systematic uncertainties

In the previous section, we have studied in detail the main sources of experimental uncertainty, coming from the imperfect measurement of the event variables. Other possible sources of experimental error are the uncertainties in the muon energy scale, the linearity for high-energy muons and the acceptance evaluation. The assessment of the effect of these uncertainties would require a detailed detector simulation, which is outside the scope of this work. We should however remark that the analysis described in the previous section displays little sensitivity to the details of the modelling of the experimental resolution and acceptance. In fact, in building the likelihood, the crucial factor is the normalization integral in the denominator of eq. (3.2). That integral is calculated with a sharp cut on the generated lepton pseudorapidity and invariant mass for events with no $P_T^{\mu^+\mu^-}$. The data selection for the particle level analysis is instead applied on leptons that have been smeared according to the detector resolution. Therefore, the acceptance of the cuts, especially the one on $m_{\mu^+\mu^-}$ edges, is reproduced in a very approximate way. Notwithstanding this fact, we observe a good agreement between the parton-level analysis and the particle level one. This gives us confidence that the additional experimental uncertainty on the λ' measurement resolution would, at worst, only marginally affect the results of our analysis. More important would be the effect of a non-linearity in the lepton energy measurement, which could simulate a deviation from the invariant-mass distribution predicted for the Standard Model. A control on the linearity at the per cent level will be needed for this analysis.

We also need to consider the theoretical uncertainties in the likelihood calculation. The likelihood function is built by weighting real events according to a theoretical cross section formula. Any discrepancy between the theoretical formula employed and reality will induce an uncertainty on the measurement of λ'. Two main sources of uncertainty can be identified: 1) the presence of higher-order corrections to the processes and 2) the parton distribution function (PDF) for the proton. We consider here the most important QCD higher-order corrections coming from radiation from initial-state quarks, which impart a transverse momentum to the lepton-lepton system. From the above discussion of the analysis, it is clear that the results show very little sensitivity to the detailed modelling of the transverse momentum distribution of the dilepton system. In fact, even for the fully generated events the likelihood was built from the pure leading order formulas, whereas the events are generated with the full PYTHIA machinery for initial-state radiation. Therefore, the experimental error quoted in the previous section implicitly includes very pessimistic assumptions on our ability to model this effect. In a real experiment, a more realistic theoretical modelling will probably be used to build the likelihood.

The second source of uncertainty is more important, since it will affect the shapes of the distribution. All the events were generated with the CTEQ4L PDF set. We have evaluated the effect of an uncertainty on PDF parametrization by performing the likelihood using sets of PDFs different from the ones used for event generation. We chose the PDFs labelled as CTEQ4A1 and CTEQ4A5, which span an extreme range between 213 and 399 MeV for the QCD parameter $\Lambda^{[4]}$. The value of $\Lambda^{[4]}$ for the set CTEQ4L is 236 MeV. We show, in figure 13, the fractional deviation of the measured λ' from the true one for the default structure functions CTEQ4L as well as for two other possible choices. The deviation for CTEQA1 is small, as expected from the small difference in $\Lambda^{[4]}$. For the set CTEQA5 the fractional difference is approximately 10% for the lowest values of λ' considered, and

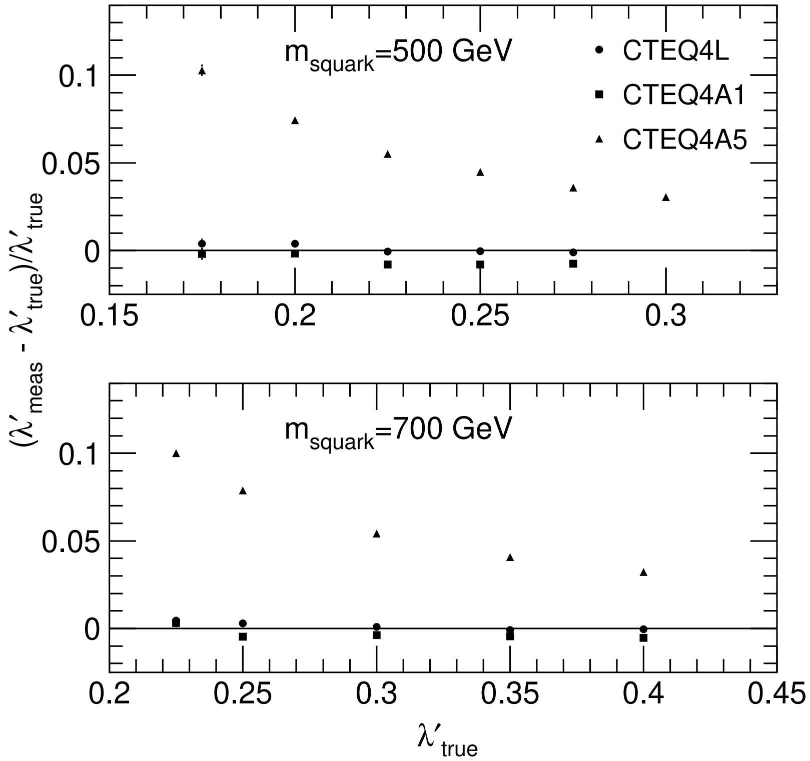

Figure 13: Fractional deviation of the measured λ' value from the true one as a function of λ' for three different choices of structure functions in the calculation of the likelihood. The events were generated with CTEQ4L. The upper plot is for $m_{\tilde{q}} = 500\,\text{GeV}$, the lower one for $m_{\tilde{q}} = 700\,\text{GeV}$.

it decreases with increasing λ' to a few per cent. We can tentatively conclude that the uncertainty on the measurement coming from the choice of PDFs will be at the few per cent level, comparable to the statistical one.

7. Effect of the $\not{R}_p$ couplings on the decays of the squarks

The above discussion establishes that the dimuon production at the LHC has enough sensitivity to $\not{R}_p$ couplings to admit their measurement with a fair accuracy. Our analysis shows that a $\not{R}_p$ coupling of the order of the gauge coupling can be measured quite accurately even for rather large squark masses, up to 700–900 GeV. Clearly, squarks in this mass range have a substantial production cross section at the LHC. So this naturally brings us to the question of whether one could detect or even measure such couplings in the decays of these squarks. A discussion of this issue is clearer if we review a few facts about the possibilities of measuring the $\not{R}_p$ couplings in collider experiments in general. These are, of course, strongly dependent on the value of the $\not{R}_p$ coupling being probed. In the worst-case scenario, it may be so small that the only effect it has is to cause the decay of the LSP and that too outside the detector, so that it is mistaken for a stable non-interacting particle. In this situation, we will altogether miss the phenomenon of R-parity violation at the colliders. For intermediate values of these couplings, one will get to a region where a significant fraction of the LSPs will decay inside the inner cavity of the LHC detector and in that case one might be able to measure the strength of these couplings by detecting the displaced vertices inside the detector. To the best of our knowledge, a detailed experimental study to map the parameter space in this case is not currently available. Then comes the range of couplings that are large enough to cause a prompt decay of the LSP, giving rise to striking final states, but are still not large enough to cause single-sparticle production or significantly affect decays of sparticles other than the LSP. In this range of values the distinctive final states caused by the decay of the LSP due to the $\not{R}_p$ couplings can provide evidence for the existence of $\not{R}_p$, but cannot give any information whatsoever on their size. And finally comes the region of the even larger $\not{R}_p$ couplings that we have considered. Here, one is sensitive to the effects of these couplings via virtual exchanges of sparticles on scattering processes as well as decays of sparticles, other than the LSP, caused by them. We have demonstrated in the above work the feasibility of "measuring" such a $\not{R}_p$ coupling through the contribution of virtual squark exchanges to the dimuon production. This offers perhaps the cleanest way of measuring the $\not{R}_p$ couplings with an adequate control of the experimental and theoretical systematic uncertainties, as the only input required for this is the squark mass. As already mentioned, for values of the squark masses under consideration, their production cross sections at the LHC are substantial. Hence, the effect of the $\not{R}_p$ couplings on the decays of the squark produced via the strong interactions needs to be studied. A particularly attractive case will be when the $\not{R}_p$ decay of the squark competes with an R_p-conserving decay with an identifiable signature. A comparison of the two can then give a direct measurement of the $\not{R}_p$ coupling. A promising example for the couplings we have considered is the $\not{R}_p$ decay $\tilde{t} \to \mu+$ jet. To study this issue, we will need to consider both the total production cross sections and the branching fractions into the various channels.

Squark pair-production has been analysed at length in various papers and depends crucially on the gluino mass. A crude summary of these results relevant to our discussion is that "for any squark lighter than approximately 800 GeV, the pair-production cross section at the LHC is large enough to lead to discovery". For the most part, the reach in mass and possibility of discovery will be independent of whether R-parity is violated or not. The measurement of the relevant coupling, or even the establishment of its identity, would, however, require that at least two channels be measurable with a relatively high degree of accuracy. One of these should be R-parity-violating, while the other should be R-conserving. For top-squarks, the presence of leptons and b-jets in the final state provides a handle for the identification of the exclusive decays of interest. The relevant R-conserving decay channels are $\tilde{q} \to q\tilde{g}$, $q\tilde{\chi}_j^0$, $q'\tilde{\chi}_j^{\pm}$, $\tilde{q}'W$. Each of these channels could lead to a cascade process culminating in a $\not{R}_p$ decay. We are, however, concerned with the $\not{R}_p$ decay of the original squark. In figure 14, we display $\not{R}_p$-branching fraction contours (into $\mu^+ + d$) for the decay of a 300 GeV stop. The assumed value of λ'_{231} is the least that would permit a detection with a statistical accuracy of 5%, if any dilution in the efficiency of the analysis from surviving backgrounds is disregarded. We see that barring very light charginos, the $\not{R}_p$ mode tends to dominate.

JHEP08(2002)004

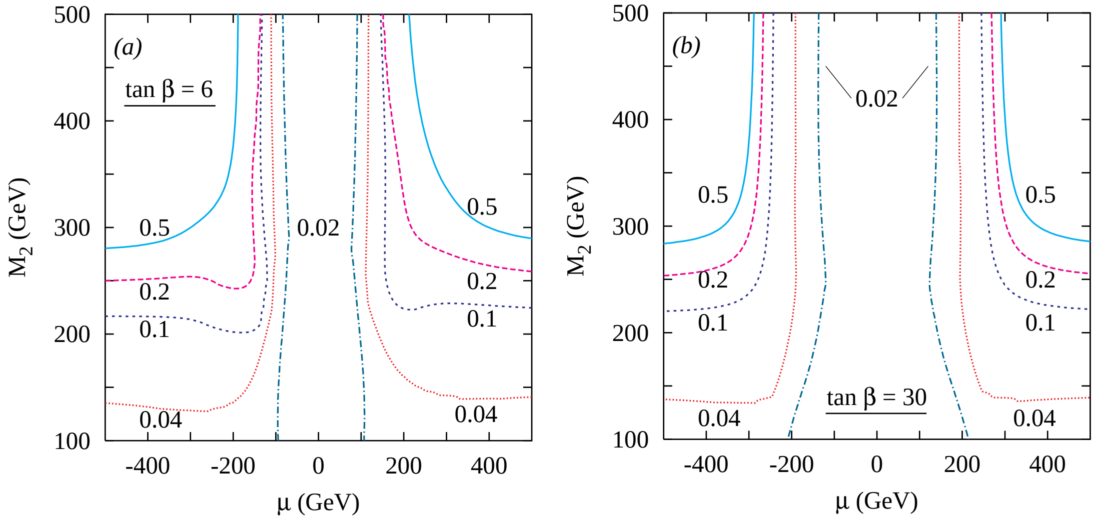

Figure 14: Contours for the branching fraction of a 300 GeV stop ($\tilde{t}_L$) into the R-parity-violating channel. The unification relation between the gaugino masses has been assumed. The value of the R-violating coupling ($\lambda'_{231} = 0.16$) is the minimum necessary for a determination λ' to an accuracy of 5% (see figure 6). The left and right panels correspond to two different values of $\tan\beta$.

An overwhelmingly large $\not{R}_p$ branching fraction, while leading to spectacular signals, is hardly amenable to a precision measurement of the coupling. Similar arguments hold for a very small $\not{R}_p$ branching fraction. The best hope is therefore for moderate values of M_2 and μ. It is thus clear that, at the level of branching ratios, stop decays would provide a sufficient number of events for the measurement of the $\not{R}_p$ coupling over a significant parameter space. A detailed experimental analysis, outside the scope of this work, is however needed to ascertain whether it will be possible to isolate the final states produced by the two relevant processes, with adequate efficiency, and with a level of purity that would permit a reasonably accurate determination of the relevant branching fractions.

8. Conclusions

To summarize, we demonstrate that an analysis of the Drell-Yan process at the LHC detectors would be a significant tool in the task of probing the parameter space in an R_p-violating supersymmetric model. While the deviation in the total cross section is at best a few per cent, even for large values of the relevant R_p-violating coupling constant, the differential distributions are much more discriminating, the distribution in the dilepton invariant mass proving particularly useful. By adopting the maximum likelihood method we could maximize the sensitivity of the measurement, avoiding at the same time the normalization uncertainties due to structure functions as well as higher-order corrections, etc.

Working, for definiteness, with dimuon production in the ATLAS detector, we showed that, for a wide range of the parameter space, R_p-violating supersymmetry would be amenable to discovery through this process. Even more importantly, a measurement of the squark mass as well as the $\not{R}_p$ coupling would be possible with relatively low errors: 2–3% for the coupling and somewhat larger for the mass. These errors could be reduced even further if additional information about the squark mass were to become available from other measurements. We found the systematic errors to be small. The analysis proved to be quite robust and the results gleaned from fully generated events were very similar to those obtained from a parton-level study. Since for the range of squark masses to which our investigation is sensitive, they can be pair-produced copiously at the LHC, we also further looked into the possibility of determining *the same* $\not{R}_p$ coupling, for which we analysed the sensitvity using the Drell-Yan process, through the decays of the squarks.

Finally, let us add that even though we have confined ourselves to dimuon production in a particular theory (namely R_p-violating supersymmetry), a similar analysis could be carried out for dielectron production equally well. In general such an analysis can be used to study effects of any alternate theories of physics, beyond the SM, which affect the Drell-Yan process. Our analysis demonstrates that such studies would complement very well the more direct methods for new particle search.

Acknowledgments

This work was initiated during a workshop held in Les Houches. We warmly thank Patrick Aurenche and all of the organizing team for the stimulating program, the excellent atmosphere and the outstanding computing facilities. We thank the ATLAS collaboration members for useful discussions. We have made use of the physics analysis framework and tools, which are the result of collaboration-wide efforts. DC thanks the Theory Division, CERN for hospitality while part of the project was being carried out and the Dept. of Science and Technology, India, for financial assistance under the Swarnajayanti Fellowship grant.

References

[1] P. Fayet, *Spontaneously broken supersymmetric theories of weak, electromagnetic and strong interactions*, *Phys. Lett.* **B 69** (1977) 489.

[2] G.R. Farrar and P. Fayet, *Phenomenology of the production, decay and detection of new hadronic states associated with supersymmetry*, *Phys. Lett.* **B 76** (1978) 575.

[3] L.E. Ibáñez and G.G. Ross, *Discrete gauge symmetries and the origin of baryon and lepton number conservation in supersymmetric versions of the standard model*, *Nucl. Phys.* **B 368** (1992) 3.

[4] B.C. Allanach and A. Dedes, *R-parity violating anomaly mediated supersymmetry breaking*, *J. High Energy Phys.* **06** (2000) 017 [hep-ph/0003222].

[5] H.K. Dreiner and G.G. Ross, *Sphaleron erasure of primordial baryogenesis*, *Nucl. Phys.* **B 410** (1993) 188 [hep-ph/9207221].

[6] CDF collaboration, T. Affolder et al., *Search for gluinos and scalar quarks in $p\bar{p}$ collisions at $\sqrt{s} = 1.8$ TeV using the missing energy plus multijets signature*, *Phys. Rev. Lett.* **88** (2002) 041801 [hep-ex/0106001];

D0 collaboration, B. Abbott et al., *Search for R-parity violating supersymmetry in the dielectron channel*, *Phys. Rev. Lett.* **83** (1999) 4476 [hep-ex/9907019];
CDF collaboration, F. Abe et al., *Search for R-parity violating supersymmetry using like-sign dielectrons in $p\bar{p}$ collisions at $\sqrt{s} = 1.8$ TeV*, *Phys. Rev. Lett.* **83** (1999) 2133 [hep-ex/9908063];
D. Choudhury and S. Raychaudhuri, *Like-sign dileptons at the fermilab Tevatron revisited in the light of the HERA high-Q^2 anomaly*, *Phys. Rev.* **D 56** (1997) 1778 [hep-ph/9703369].

[7] D. Choudhury and S. Raychaudhuri, *R-parity violation at HERA?*, *Phys. Lett.* **B 401** (1997) 54 [hep-ph/9702392];
G. Altarelli, J.R. Ellis, G.F. Giudice, S. Lola and M.L. Mangano, *Pursuing interpretations of the HERA large-Q^2 data*, *Nucl. Phys.* **B 506** (1997) 3 [hep-ph/9703276];
H.K. Dreiner and P. Morawitz, *High Q^2-anomaly at HERA and supersymmetry*, *Nucl. Phys.* **B 503** (1997) 55 [hep-ph/9703279];
J. Kalinowski, R. Ruckl, H. Spiesberger and P.M. Zerwas, *Leptoquark/squark interpretation of HERA events: virtual effects in e^+e^- annihilation to hadrons*, *Z. Physik* **C 74** (1997) 595 [hep-ph/9703288];
T. Kon and T. Kobayashi, *Stops in R-parity breaking model for high-Q^2 events at HERA*, *Phys. Lett.* **B 409** (1997) 265 [hep-ph/9704221];
G. Altarelli, G.F. Giudice and M.L. Mangano, *What if charged current events at large Q^2 are observed at HERA?*, *Nucl. Phys.* **B 506** (1997) 29 [hep-ph/9705287];
J.R. Ellis, S. Lola and K. Sridhar, *Pursuing the strange stop interpretation of the HERA large-Q^2 data*, *Phys. Lett.* **B 408** (1997) 252 [hep-ph/9705416];
M. Carena, D. Choudhury, S. Raychaudhuri and C.E.M. Wagner, *Supersymmetry and charged current events at HERA*, *Phys. Lett.* **B 414** (1997) 92 [hep-ph/9707458].

[8] H1 collaboration, C. Adloff et al., *Observation of events at very high Q^2 in ep collisions at HERA*, *Z. Physik* **C 74** (1997) 191 [hep-ex/9702012];
ZEUS collaboration, J. Breitweg et al., *Comparison of Zeus data with standard model predictions for $e^+p \to e^+X$ scattering at high x and Q^2*, *Z. Physik* **C 74** (1997) 207 [hep-ex/9702015].

[9] V.D. Barger, G.F. Giudice and T. Han, *Some new aspects of supersymmetry R-parity violating interactions*, *Phys. Rev.* **D 40** (1989) 2987.

[10] G. Bhattacharyya and D. Choudhury, *D and tau decays: placing new bounds on R-parity violating supersymmetric coupling*, *Mod. Phys. Lett.* **A 10** (1995) 1699 [hep-ph/9503263].

[11] Some studies are:
R.M. Godbole, P. Roy and X. Tata, *Tau signals of R-parity breaking at LEP200*, *Nucl. Phys.* **B 401** (1993) 67 [hep-ph/9209251];
A.S. Joshipura, V. Ravindran and S.K. Vempati, *Neutrino mass constraints on R violation and HERA anomaly*, *Phys. Lett.* **B 451** (1999) 98 [hep-ph/9706482];
M. Drees, S. Pakvasa, X. Tata and T. ter Veldhuis, *A supersymmetric resolution of solar and atmospheric neutrino puzzles*, *Phys. Rev.* **D 57** (1998) 5335 [hep-ph/9712392];
E.J. Chun and J.S. Lee, *Implication of super-Kamiokande data on R-parity violation*, *Phys. Rev.* **D 60** (1999) 075006 [hep-ph/9811201];
A. Abada and M. Losada, *Constraints on a general 3-generation neutrino mass matrix from neutrino data: application to the MSSM with R-parity violation*, *Nucl. Phys.* **B 585** (2000) 45 [hep-ph/9908352];

A.S. Joshipura, R.D. Vaidya and S.K. Vempati, *Neutrino anomalies in gauge mediated model with trilinear R violation*, *Phys. Rev.* **D 65** (2002) 053018 [hep-ph/0107204];
F. Borzumati and J.S. Lee, *Novel constraints on $\Delta L = 1$ interactions from neutrino masses*, hep-ph/0207184.

[12] Heidelberg-Moscow collaboration, H. Klapdor-Kleingrothaus et al., *Double β decay and neutrino mass: the Heidelberg-Moscow experiment*, *Prog. Part. Nucl. Phys.* **32** (1994) 261;
J.W.F. Valle, *Neutrino-less double beta decay and physics beyond the standard model*, hep-ph/9509306;
G. Bhattacharyya, H.V. Klapdor-Kleingrothaus and H. Pas, *Neutrino mass and magnetic moment in supersymmetry without R-parity in the light of recent data*, *Phys. Lett.* **B 463** (1999) 77 [hep-ph/9907432].

[13] For a summary of these limits, see for example, B.C. Allanach, A. Dedes and H.K. Dreiner, *Bounds on R-parity violating couplings at the weak scale and at the SUSY scale*, *Phys. Rev.* **D 60** (1999) 075014 [hep-ph/9906209];
G. Bhattacharyya, *A brief review of R-parity violating couplings*, talk given at *Workshop on physics beyond the Standard Model: beyond the desert: accelerator and nonaccelerator approaches*, Tegernsee, Germany, 8-14 June 1997 [hep-ph/9709395].

[14] E.A. Baltz and P. Gondolo, *Neutralino decay rates with explicit R-parity violation*, *Phys. Rev.* **D 57** (1998) 2969 [hep-ph/9709445];
H.K. Dreiner, P. Richardson and M.H. Seymour, *Parton-shower simulations of R-parity violating supersymmetric models*, *J. High Energy Phys.* **04** (2000) 008 [hep-ph/9912407];
F. Borzumati, R.M. Godbole, J.L. Kneur and F. Takayama, *Lightest-neutralino decays in R_p-violating models with dominant λ' and λ couplings*, *J. High Energy Phys.* **07** (2002) 037 [hep-ph/0108244].

[15] S. Dawson, *R-parity breaking in supersymmetric theories*, *Nucl. Phys.* **B 261** (1985) 297.

[16] F. Borzumati, J.-L. Kneur and N. Polonsky, *Higgs-strahlung and R-parity violating slepton-strahlung at hadron colliders*, *Phys. Rev.* **D 60** (1999) 115011 [hep-ph/9905443];
G. Moreau, E. Perez and G. Polesello, *Resonant sneutrino production in supersymmetry with R-parity violation at the LHC*, *Nucl. Phys.* **B 604** (2001) 3 [hep-ph/0003012];
H.K. Dreiner, P. Richardson and M.H. Seymour, *Resonant slepton production in hadron hadron collisions*, *Phys. Rev.* **D 63** (2001) 055008 [hep-ph/0007228];
D. Choudhury, S. Majhi and V. Ravindran, *QCD corrections to resonant slepton production in hadron colliders*, hep-ph/0207247.

[17] D.K. Ghosh, S. Raychaudhuri and K. Sridhar, *Bounds from $t\bar{t}$ production on R-parity violating models of supersymmetry*, *Phys. Lett.* **B 396** (1997) 177 [hep-ph/9608352].

[18] T. Han and M.B. Magro, *Top quark decay via R-parity violating interactions at the Tevatron*, *Phys. Lett.* **B 476** (2000) 79 [hep-ph/9911442];
K.J. Abraham, K. Whisnant, J.M. Yang and B.-L. Young, *Probing R-violating top quark decays at hadron colliders*, *Phys. Rev.* **D 63** (2001) 034011 [hep-ph/0007280].

[19] G. Bhattacharyya, D. Choudhury and K. Sridhar, *R-parity violating SUSY or leptoquarks: virtual effects in dilepton production*, *Phys. Lett.* **B 349** (1995) 118 [hep-ph/9412259].

[20] J. Kalinowski, R. Rückl, H. Spiesberger and P.M. Zerwas, *R-parity violating SUSY signals in lepton pair production at the Tevatron*, *Phys. Lett.* **B 414** (1997) 297 [hep-ph/9708272].

[21] J.L. Hewett and T.G. Rizzo, *Much ado about leptoquarks: a comprehensive analysis*, *Phys. Rev.* **D 56** (1997) 5709 [hep-ph/9703337].

[22] E.L. Berger, B.W. Harris and Z. Sullivan, *Direct probes of R-parity-violating supersymmetric couplings via single-top-squark production*, *Phys. Rev.* **D 63** (2001) 115001 [hep-ph/0012184];
K.-I. Hikasa, J.M. Yang and B.-L. Young, *R-parity violation and top quark polarization at the Fermilab Tevatron collider*, *Phys. Rev.* **D 60** (1999) 114041 [hep-ph/9908231];
D. Choudhury, *Leptoquark search at e^+e^- colliders*, *Phys. Lett.* **B 346** (1995) 291 [hep-ph/9408250];
A. Datta, *Effects of lepton number violating interactions on $t\bar{t}$ production at NLC*, *Phys. Rev.* **D 65** (2002) 054019 [hep-ph/0108150].

[23] R. Hamberg, W.L. van Neerven and T. Matsuura, *A complete calculation of the order α_s^2 correction to the Drell-Yan K factor*, *Nucl. Phys.* **B 359** (1991) 343;
R.V. Harlander and W.B. Kilgore, *Next-to-next-to-leading order Higgs production at hadron colliders*, *Phys. Rev. Lett.* **88** (2002) 201801 [hep-ph/0201206].

[24] W. Beenakker et al., *The production of charginos/neutralinos and sleptons at hadron colliders*, *Phys. Rev. Lett.* **83** (1999) 3780 [hep-ph/9906298].

[25] The simultaneous presence of more than one $\not{R}_p$ coupling could potentially lead to flavour-changing neutral currents. The consequent stringent limits on such products of couplings have been derived in:
K. Agashe and M. Graesser, *r-parity violation in flavor changing neutral current processes and top quark decays*, *Phys. Rev.* **D 54** (1996) 4445 [hep-ph/9510439];
D. Choudhury and P. Roy, *New constraints on lepton nonconserving R-parity violating couplings*, *Phys. Lett.* **B 378** (1996) 153 [hep-ph/9603363];
A.Y. Smirnov and F. Vissani, *Upper bound on all products of R-parity violating couplings λ' and λ'' from proton decay*, *Phys. Lett.* **B 380** (1996) 317 [hep-ph/9601387].

[26] T. Sjöstrand, *High-energy physics event generation with Pythia 5.7 and Jetset 7.4*, *Comput. Phys. Commun.* **82** (1994) 74.

[27] E. Richter-Was, D. Froidevaux and L. Poggioli, *ATLFAST 2.0: a fast simulation package for ATLAS*, ATLAS Internal Note ATL-PHYS-98-131 1998.

[28] G.J. Feldman and R.D. Cousins, *Phys. Rev.* **D 57** (1998) 3873 [physics/9711021].

[29] ATLAS collaboration, *ATLAS detector and physics performance technical design report*, ATLAS TDR 15, CERN/LHCC/99-15 1999.

[30] B.C. Allanach et al., *Measuring supersymmetric particle masses at the LHC in scenarios with baryon-number R-parity violating couplings*, *J. High Energy Phys.* **03** (2001) 048 [hep-ph/0102173].

[31] J.C. Collins and D.E. Soper, *Angular distribution of dileptons in high-energy hadron collisions*, *Phys. Rev.* **D 16** (1977) 2219.

JHEP08(2002)004